

Topside Ionosphere as seen by Swarm GPS

Introduction

The topside ionosphere, usually defined as the part of the ionospheric F layer which is located above the peak density, is difficult to monitor using ground-based observations. LEO missions like Swarm, GOCE, GRACE, and the Sentinels give insight into these altitudes. As many LEO missions, they are equipped with dual-frequency GPS receivers, which are used for precise orbit determination (POD), but may also be used for slant TEC computation.

We will show how the Swarm GPS receiver is susceptible to strong gradients in electron density, how ionospheric plasma irregularities may be detected using the GPS phase observables and how large the electron content of the plasmasphere may become in Swarm Slant TEC. Eventually we will show an example for ionospheric tomography and how the observation specific weights from the orbit determination are used to improve ionospheric tomography

Detecting Bubbles in GPS Phase measurements

A different kind of uncertainties in the GPS phase observables may be caused by ionospheric irregularities, namely plasma bubbles. When encountering a plasma bubble the GPS phase observables get scattered. Usually, the ROTI approach is used, but because of the high dynamics of the slant TEC, it has to be detrended. For that reason, we use a 31 s time window and perform a quadratic polynomial fit. Then we use the residuals to this fit and perform the ROTI approach (Figure 4). Eventually, an empirical threshold of 0.1 TECU was determined.

When comparing the irregularities found in the GPS phase observables to the provided Ionospheric Bubble Index (IBI) Product, we may see a good agreement. However, due to the tracking of different GPS satellites simultaneously, the GPS derived bubble index also contains additional information about the direction and shape of the bubble. Performing a climatological comparison, the agreement is also confirmed (Figure 5). A GPS-derived Bubble Index also has the advantage, that the approach can be applied to other LEO missions, which do not have high precision magnetometers and Langmuir Probes, but a 1 Hz GPS receiver, like GOCE or Sentinel 3A. Two results are shown in Fig. 5. As expected, for Sentinel 3A almost no irregularities are reported due to the high altitude. For GOCE however, also a large number of irregularities is reported, because of an altitude of only 250 km.

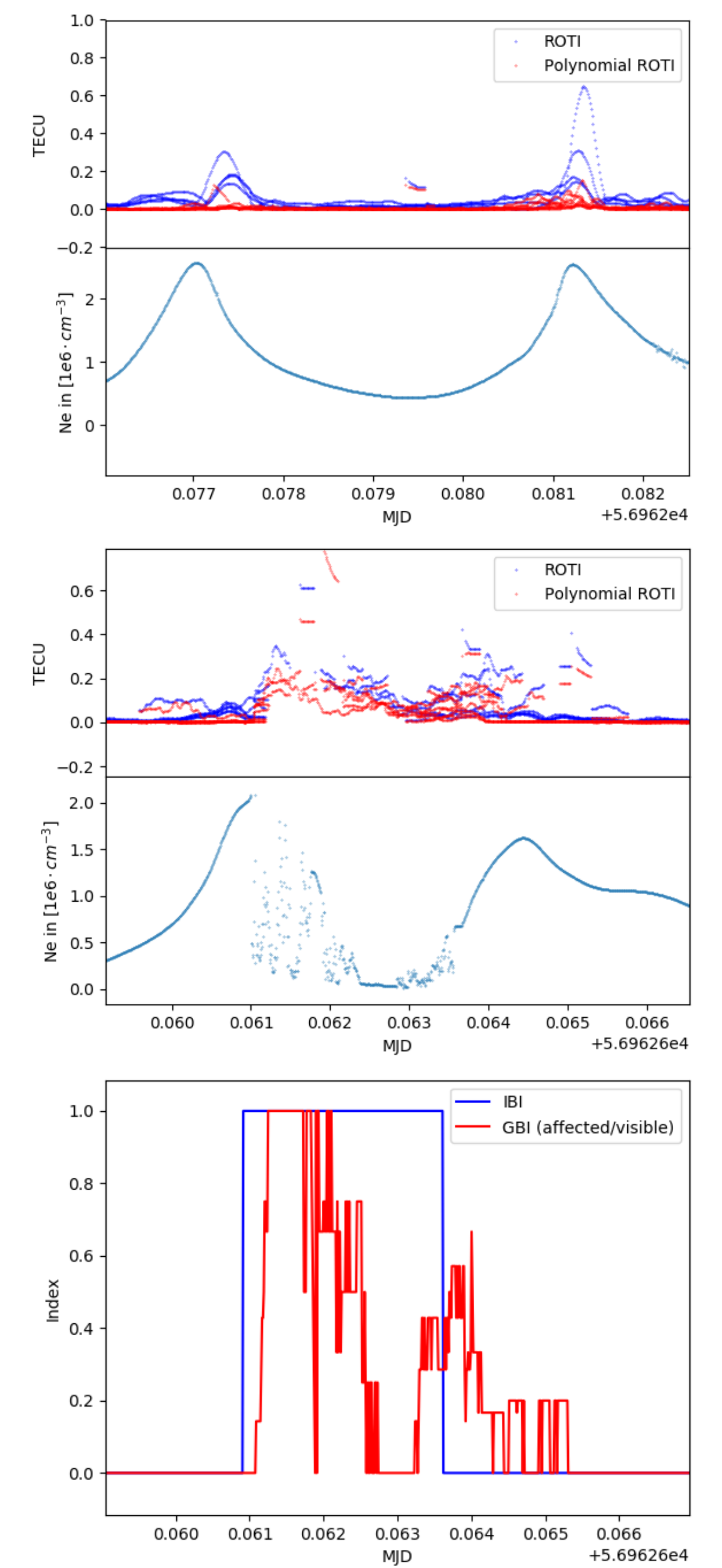


Figure 4: Quadratic ROTI compared to polynomial ROTI and measured plasma density for quiet (top) and disturbed epochs (mid). Bottom IBI compared to IBI for the disturbed epochs.

Ionosphere in Swarm GPS only gravity fields

In Swarm GPS-only gravity field computation systematic errors have been observed near the geomagnetic equator, Jäggi et al. (2016) (Figure 2).

These systematic errors are already visible on orbit level when comparing the Swarm A kinematic orbit to a reduced-dynamic orbit (Figure 1). These errors come from systematic errors in the GPS phase observables. By construction the ionosphere should not be visible in the orbits in this extent, since for POD the ionosphere-free linear combination is used.

To mitigate the impact of these errors, screening and weighting methods have been developed (Schreiter et al. 2019). These methods are based on the geometry-free linear combination, which to first order is proportional to the slant TEC:

$$L_{gf} = L_1 - L_2$$

$$sTEC \approx \frac{1}{40.3} \cdot \left(\frac{f_1^2 f_2^2}{f_1^2 - f_2^2} \right) (L_2 - L_1)$$

The most successful approach was a combination of the second time derivative with weighting based on the Rate Of TEC Index (ROTI) using a 31 s window, Figure 3.

$$ROTI = \sqrt{\frac{\langle \Delta TEC^2 \rangle - \langle \Delta TEC \rangle^2}{\Delta t}}$$

$$\sigma_{ROTI}^2 = \max(1, 60 \cdot ROTI)$$

$$\sigma_{d2}^2 = \begin{cases} 1, & \text{if } d^2/dt^2 L_{gf} < 0.025 \text{ cm/s}^2 \\ 21, & \text{if } d^2/dt^2 L_{gf} \geq 0.025 \text{ cm/s}^2 \end{cases}$$

$$\sigma^2 = \max(\sigma_{ROTI}^2, \sigma_{d2}^2)$$

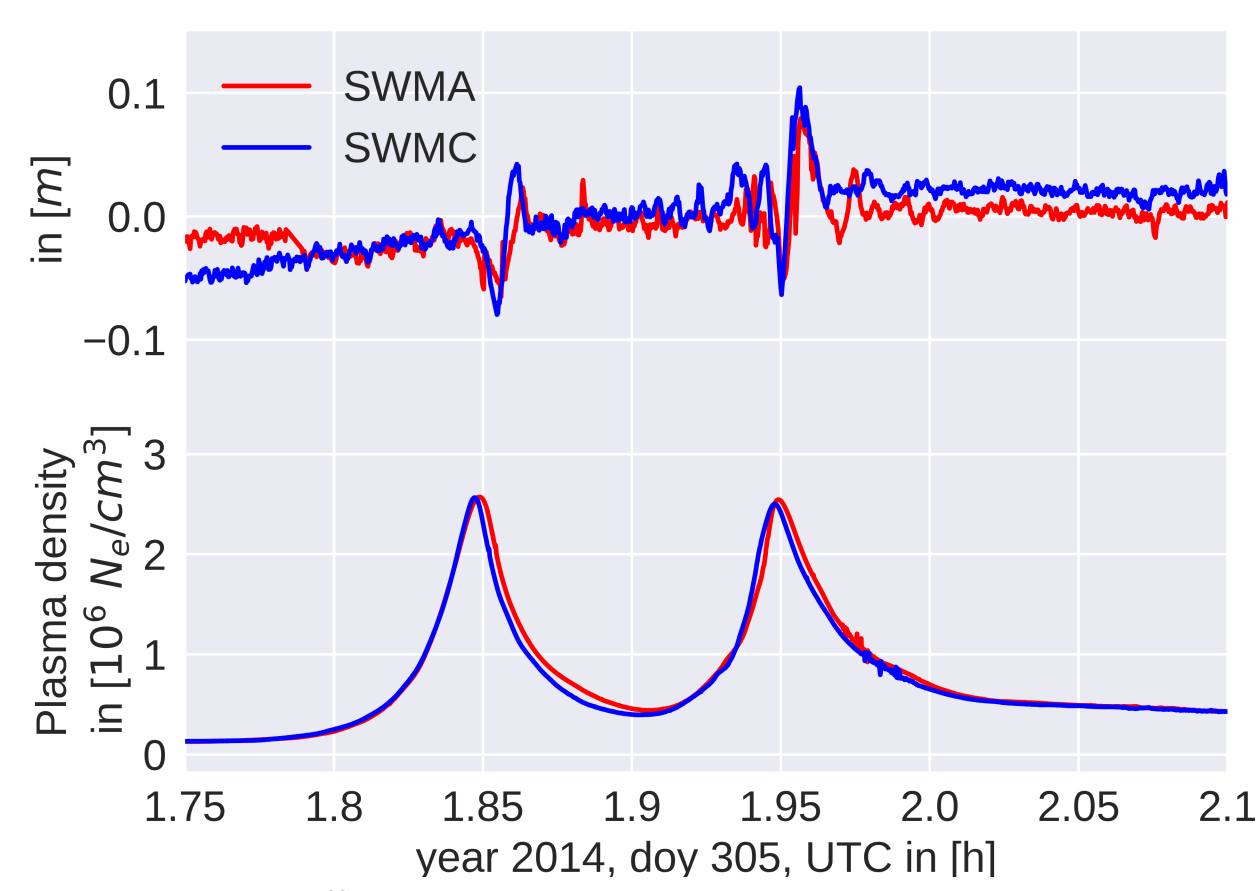


Figure 1: Differences between a Swarm kinematic and reduced dynamic orbit compared to plasma density obtained by Swarm Langmuir probes.

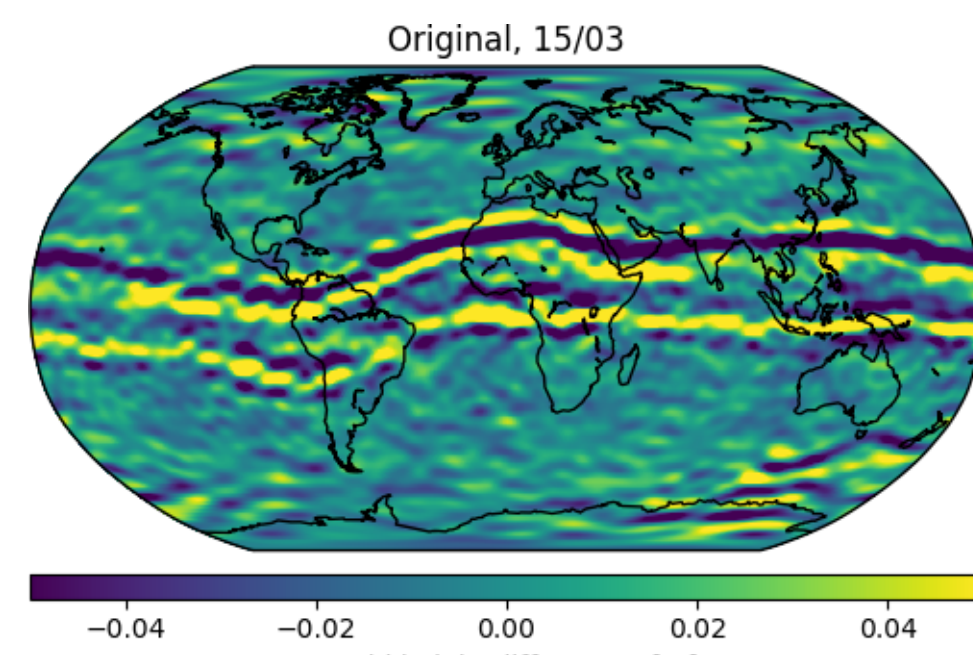


Figure 2: Geoid height differences between the unweighted Swarm GPS only gravity field solution and the JPL GRACE solution

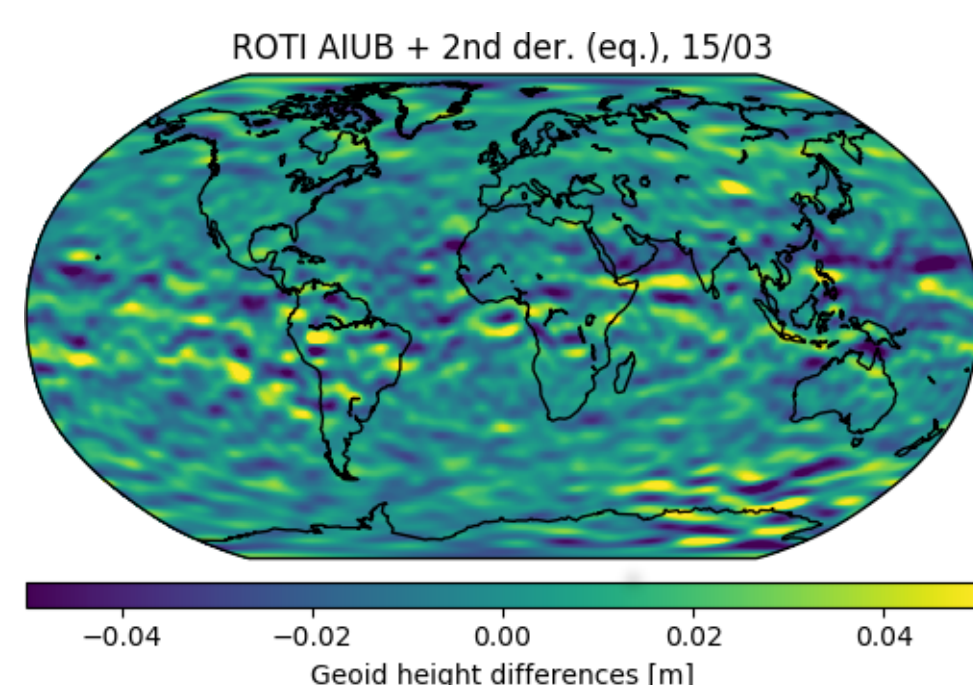


Figure 3: Geoid height differences between the weighted Swarm GPS only gravity field solution and the JPL GRACE solution

Ionospheric Tomography Using Weighting

To simplify the tomographic approach and to reduce the dimension of the grid, we first remove the plasmaspheric electron content (1000 km to 2000 km) from the Swarm sTEC observations. The plasmaspheric electron density is modeled using Sentinel sTEC observations. The model uses the electron density at 1000 km and two scale heights for below and above 2000 km, all represented by a spherical harmonics expansion.

For this example a day is chosen, where the local times of Swarm are close to the local times of Sentinel. For day 130, year 2017 the local times of Swarm are 9/21 LT, whereas the local times of Sentinel are 6/18 LT and 10/22 LT. The plasmaspheric electron content in Swarm sTEC is then removed by evaluating the model using line-of-sight integration from 1000 km to GPS altitude. The difference between the sTEC values is shown in Figure 6. For details on the model we refer to the poster of Schreiter et al., EGU General Assembly 2019.

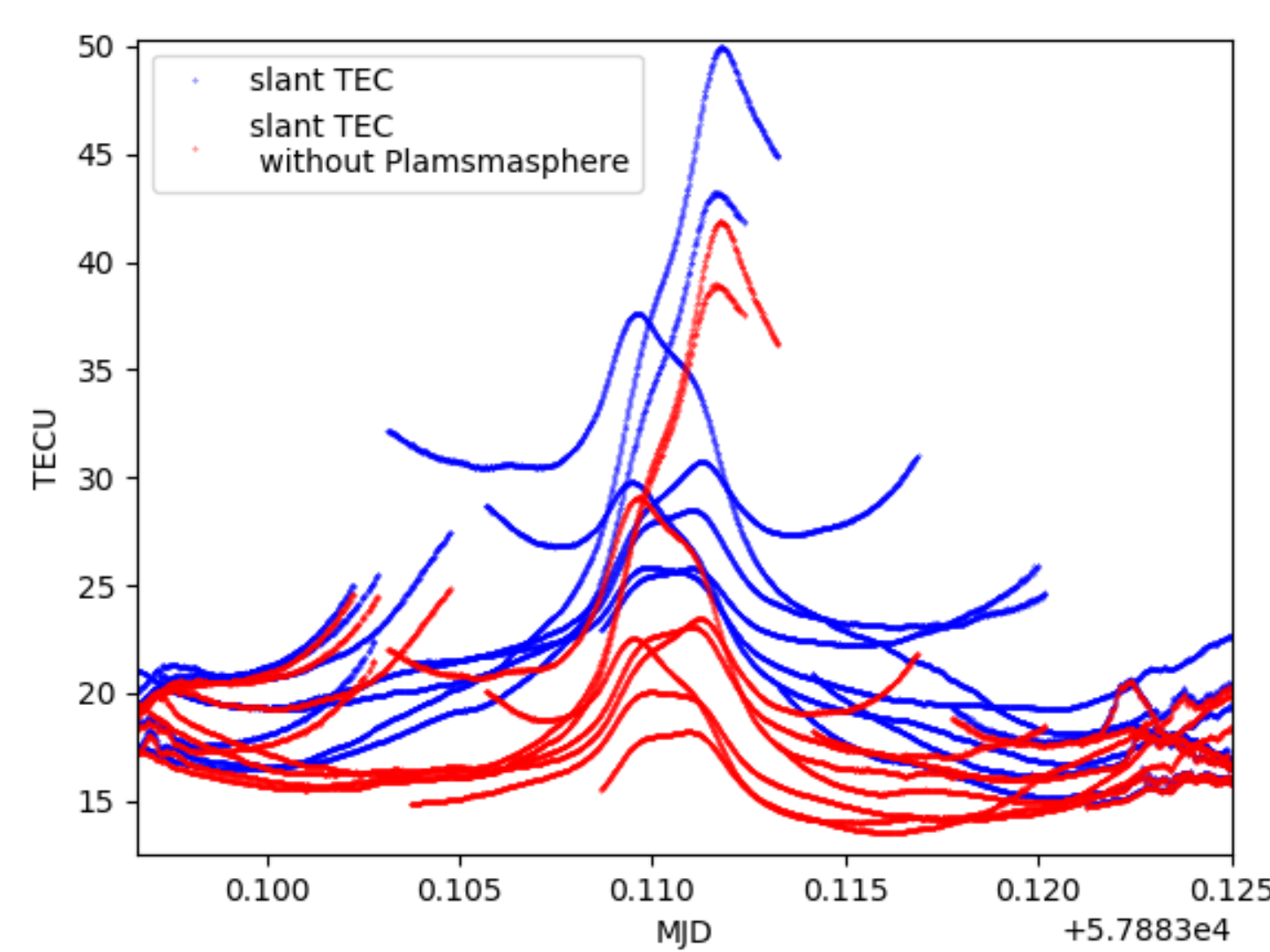


Figure 6: Swarm slant TEC with and without plasmaspheric electron content.

The ionospheric tomography is performed using a multistep procedure based on approximately 25 minutes of GPS phase data and plasma density measurements. First the area of interest is discretized in altitude (60 steps) and latitude (120 steps (0.5°)). Then the integral equation is approximated by the weighted sum of the pixel density:

$$sTEC = \int_{LEO}^{GPS} N_e dl + C_{ARC} \approx \sum_{i=0}^N l_i(N_e)_i + C_{ARC}$$

Furthermore, the lower boundary is constrained to the corrected insitu Langmuir probe densities (see Lomidze et al. 2018) and additional constraints are applied, to ensure the smoothness of the reconstruction and to avoid unrealistic values. With the conditions a prior solution is computed in a least squares adjustment with regularization:

$$\|P(Ax - y)\| + \lambda \|Bx\| \rightarrow \min.$$

Eventually the design matrix and the matrix containing the inner constraints as well as the prior solution is further refined using a modified multiplicative algebraic reconstruction technique (MART) algorithm. The MART algorithms only support positive values of x and positive entries in the matrices. Therefore, the matrix containing the constraints (C=B^TB) needs to be decomposed into a positive (C⁺) and a negative part (C⁻).

$$x_j^{k+1} = x_j^k \cdot \prod_{i=1}^m \left(\frac{y_i}{(Ax^k)_i} \right)^{\lambda A_{i,j} / \|A_{i,j}\|} \prod_{i=1}^k \left(\frac{(-C^- x^k)_i}{(C^+ x^k)_i} \right)^{\lambda C_{i,j}^+ / \|C_{i,j}^+\|}$$

The results are shown in Figure 7. When applying the MART algorithm more details become visible and the unrealistically large values in higher altitudes become smaller, but also the MART is sensitive to artifacts (mid), which may be seen, when adopting the weight matrix (bottom) and these artifacts virtually disappear.

Conclusions

Even if the Swarm POD GPS data has known artifacts it provides detailed information on the topside ionosphere. Small sTEC fluctuations can be reliably observed and may be used to generate a GPS based bubble index. Because of the existing IBI product, it is possible to directly validate the approach and transfer it to other LEO's like GOCE and Sentinel 3A. This may offer a new opportunity to study ionospheric plasma bubbles using LEO GPS receiver.

Tomographic approaches can be applied using Swarm GPS if known artifacts in the data are carefully mitigated using weighting schemes.

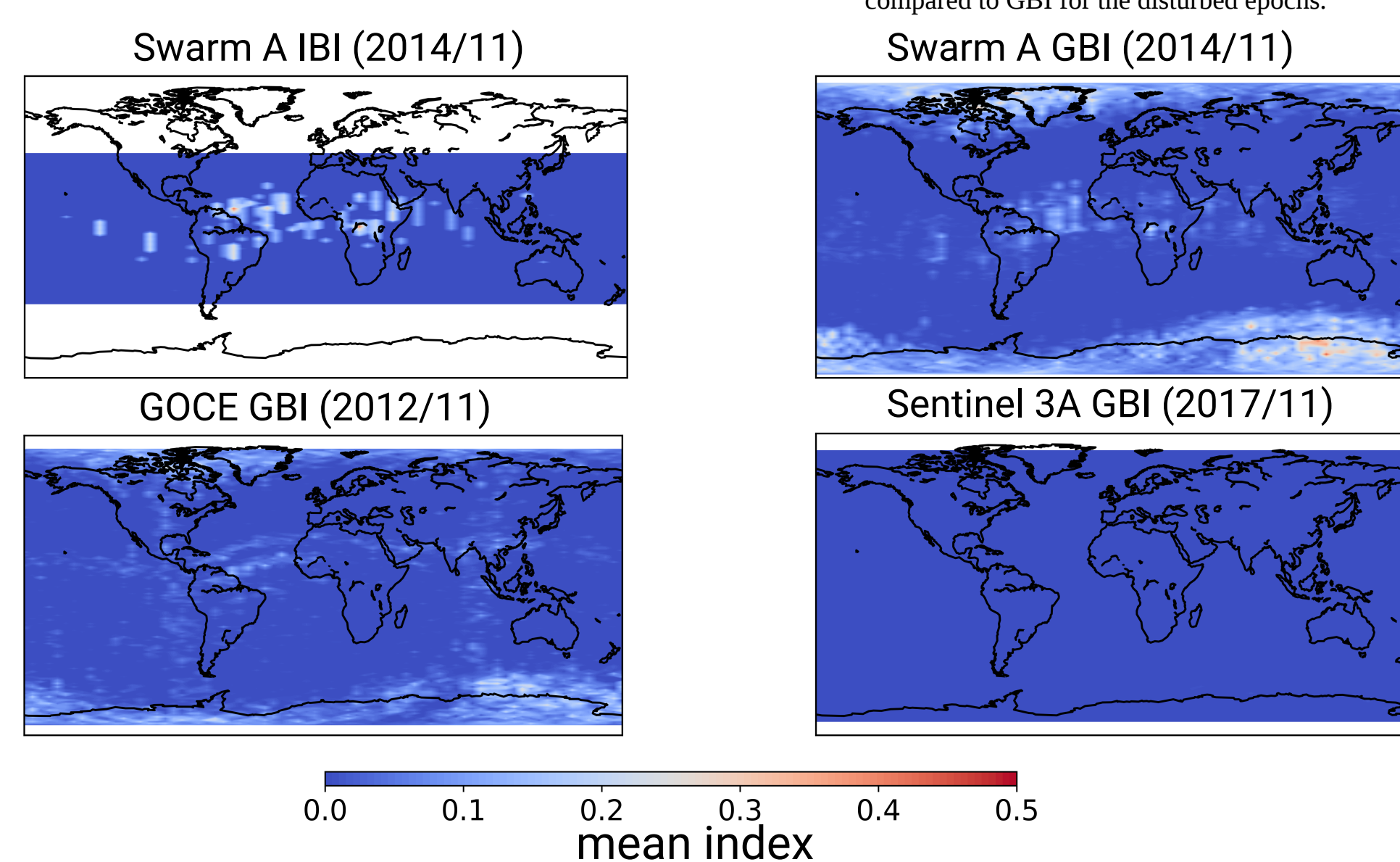


Figure 5: Binned monthly means for IBI and GBI for Swarm, GOCE and Sentinel 3A.

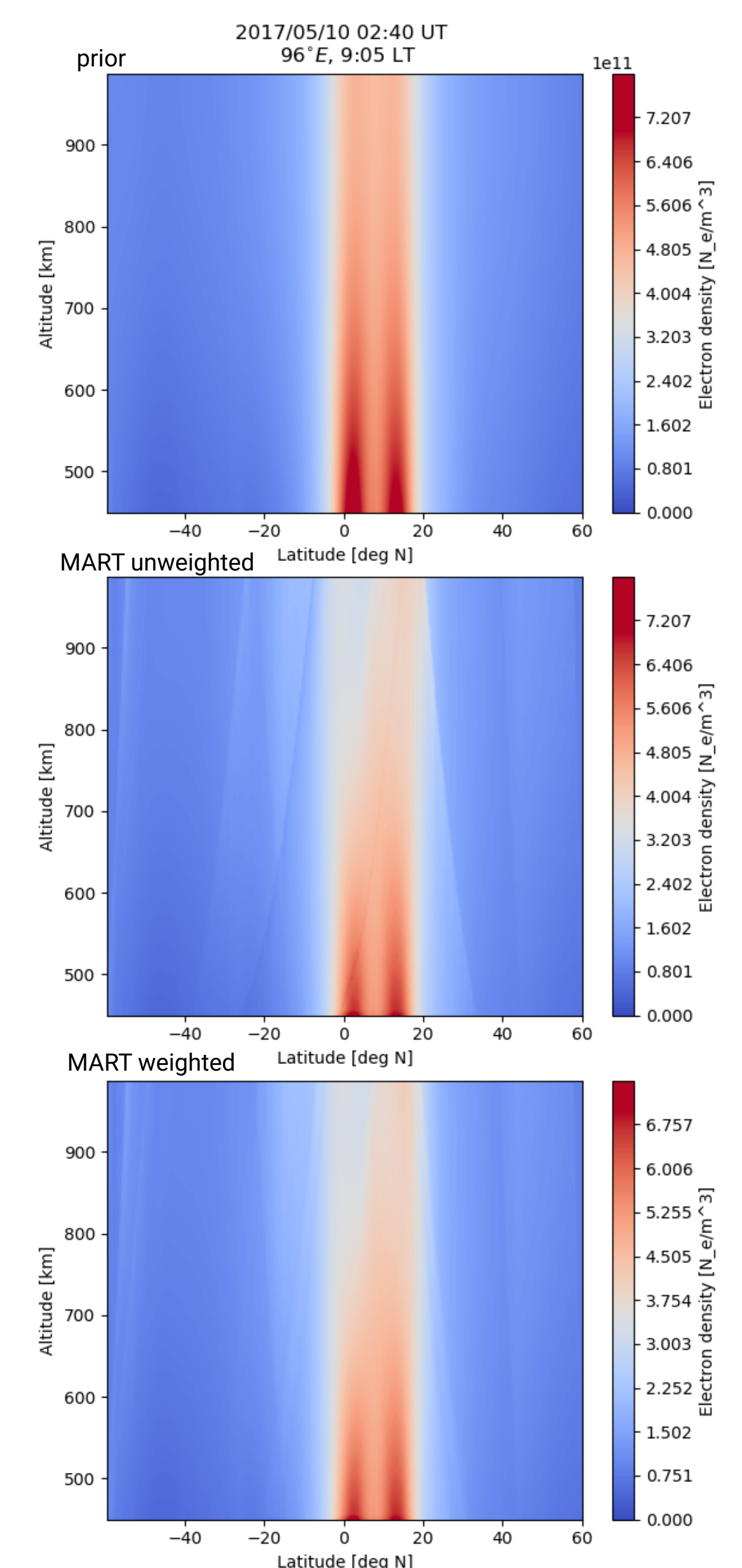


Figure 7: Ionospheric reconstruction, prior (top), MART unweighted (mid) and MART weighted (bottom)

References

- Jäggi, A., C. Dahle, D. Arnold, H. Bock, U. Meyer, G. Beutler, J. van den IJssel; 2016: Swarm kinematic orbits and gravity fields from 18 months of GPS data. *Advances in Space Research*, vol. 57 (1), pp. 218-233. DOI 10.1016/j.asr.2015.10.035;
- Schreiter, L., D. Arnold, V. Sterke, A. Jäggi; 2019: Mitigation of ionospheric signatures in Swarm GPS gravity field estimation using weighting strategies. *Ann. Geophys.*, 37, pp 111-127, 2019. DOI 10.5194/angeo-37-111-2019
- Lomidze, L., Knudsen, D. J., Burchill, J., Kouznetsov, A., & Buchert, S. C. (2018). Calibration and validation of Swarm plasma densities and electron temperatures using ground-based radars and satellite radio occultation measurements. *Radio Science*, 53, 15–36. DOI 10.1002/2017RS006415
- Schreiter, L., L. Scherliess, C. Stoller, D. Arnold, A. Jäggi; 2019: Empirical modeling of the topside ionosphere and plasmasphere using LEO GPS-TEC. EGU General Assembly 2019, Vienna, Austria, April 07-12, 2019. <http://www.berne.unibe.ch/publist/publist.php>

Contact address

Lucas Schreiter
Astronomical Institute, University of Bern
Sidlerstrasse 5
3012 Bern (Switzerland)
lucas.schreiter@aiub.unibe.ch

